UCSF
UC San Francisco Previously Published Works

Title

Identification of intra-individual variation in intracranial arterial flow by MRI and the effect on computed hemodynamic descriptors

Permalink

https://escholarship.org/uc/item/1qm5954f

Journal

Magnetic Resonance Materials in Physics, Biology and Medicine, 34(5)

ISSN

0968-5243

Authors

Liu, Xinke
Kao, Evan
Haraldsson, Henrik
et al.

Publication Date

2021-10-01

DOI

10.1007/s10334-021-00917-0

Peer reviewed

eScholarship.org Powered by the California Digital Library
University of California

Author Manuscript

Author Manuscript

Author Manuscript

Author Manuscript

HHS Public Access

Author manuscript

MAGMA. Author manuscript; available in PMC 2022 October 01.

Published in final edited form as:

MAGMA. 2021 October ; 34(5): 659–666. doi:10.1007/s10334-021-00917-0.

Identification of Intra-Individual Variation in Intracranial Arterial Flow by MRI and the Effect on Computed Hemodynamic Descriptors

Xinke Liu, MD[1,2], **Evan Kao, PhD**[2], **Henrik Haraldsson, PhD**[2], **Megan Ballweber, MS**[2], **Alastair Martin, PhD**[2], **Youxiang Li, MD**[1,#], **Yuting Wang, MD**[2,3,#], **David Saloner, PhD**[2]

[1]Department of Interventional Neuroradiology, Beijing Neurosurgical Institute and Beijing Tiantan Hospital, Capital Medical University, Beijing, China

[2]Department of Radiology and Biomedical Imaging, University of California San Francisco, San Francisco, United States

[3]Department of Radiology, Sichuan Academy of Medical Sciences and Sichuan Provincial People's Hospital, Chengdu, China

Abstract

Objectives: To determine the intra-individual flow variation in serially acquired studies, and the influence of this variation on subsequent hemodynamic simulations using the inlet flow as a boundary condition.

Materials and Methods: This prospective study included 51 patients (37 females and 14 males) with unruptured intracranial aneurysms who have received more than 3 times follow-up of 2D phase-contrast MR. The flow and velocity parameters were extracted to calculate the reproducibility and variation. Patient-specific computational fluid dynamics simulations were performed using the measured flows.

Results—Intraclass correlation coefficients for mean and maximum velocity and flow parameters ranged from 0.77 to 0.90. A 10% CV of mean flow was identified. Variations of 10% in inlet flow resulted in hemodynamic changes including 41.41% of peak systolic wall shear stress; 39.13% of end diastolic wall shear stress; 2.79% of low shear area at peak systole; 2.12% of low shear area at end diastole: 47.57% of time-averaged wall shear stress; and 0.17% of oscillatory shear index.

Conclusion: This study identified 10% of intra-individual mean flow variation on phase-contrast MR. Intra individual flow variation resulted in a non-negligible variation in wall shear stress, but relatively small variation in low shear area in hemodynamic calculations.

[#]Corresponding Author: Youxiang Li, liyouxiang@263.net, Telephone: (510) 982-1909, Yuting Wang, wangyuting_330@163.com, Telephone: (415) 750-2238, Youxiang Li and Yuting Wang are co-corresponding author in this paper.

Authors' contributions

Study conception and design: David Saloner, Xinke Liu, Yuting Wang, Youxiang Li

Acquisition of data: Henrik Haraldsson, Megan Ballweber, Alastair Martin

Analysis and interpretation of data: Xinke Liu, Evan Kao, Yuting Wang

Drafting of manuscript: Xinke Liu

Critical revision: David Saloner

Author Manuscript Author Manuscript Author Manuscript Author Manuscript

Keywords

MR; intracranial; flow; hemodynamics; reproducibility

Introduction

The worldwide prevalence of intracranial aneurysm disease is estimated to be 3.2% (95% [CI], 1.9%–5.2%) [1]. Intracranial aneurysms are characterized by high morbidity and mortality rates following rupture[2,3]. It is generally considered that hemodynamics plays a critical role in aneurysm development and rupture[4–6]. While computational fluid dynamics (CFD) studies have the potential to provide important insights into the mechanisms of aneurysm development and rupture, there remains concern as to the poor consistency of CFD results[7]. Several assumptions are commonly made when conducting CFD simulations of flow in intracranial aneurysms, specifically that vascular compliance is negligible, that flow is laminar, and that blood viscosity is Newtonian. These assumptions have been shown to be reasonable[8,9], and with those assumptions, the accuracy of CFD rests only on an accurate definition of the geometry of the lumenal surface, and of the inlet flow waveform.

The error in geometry segmentation and its effect on hemodynamics has been explored elsewhere[10,11]. However, the dependence of hemodynamic descriptors on the inlet flow waveform boundary condition is less well established. Many investigators use generalized or idealized flow waveforms[12], and when patient-specific flow rates are used, little attention is paid to measurement variability. Blood flow in the supplying vessels of the brain can be measured using phase-contrast MR (PCMR). PCMR enables the acquisition of geometry and flow information simultaneously[13]. This technique is also noninvasive, and does not require exposure to radiation or contrast material[14].

There is little data on serial studies of intracranial flow in the same patients as patient-specific flow conditions are rarely assessed as part of the routine clinical examination. de Verdier et.al performed a test-retest measurement on a relatively small sample size[15]. However, that study only included healthy volunteers and therefore did not account for the variability that might be expected in patients with vascular disease that include: variations from making measurements at different locations along the feeding artery; and increased physiological variability. These physiological factors are confounded by reader errors in postprocessing and analysis with delineation of the lumenal contour being a factor of major concern.

As noted above, it is important to understand the reproducibility of measurement of the inlet flow waveform in assessing the value of CFD in predicting vascular disease progression. This study was limited to the evaluation of patients with known but untreated intracranial aneurysms. To measure the variation of PCMR that is generally encountered in patients with vascular disease, we carried out a longitudinal study in unruptured intracranial aneurysm patients with multiple follow-up scans. We further investigated the effect that likely uncertainties in flow measurement would have on computed hemodynamic metrics.

Author Manuscript Author Manuscript Author Manuscript Author Manuscript

Material and method

Patient Selection

A cohort of patients with intracranial aneurysms were recruited and scanned from April 2005 to January 2013. Inclusion criteria included: diagnosis of at least one unruptured intracranial aneurysm, and the ability to undergo an MR study. Exclusion criteria included: metal implants, claustrophobia, or a known allergic reaction to the MR contrast agent. This study was conducted under IRB approval. All subjects involved gave informed written consent for study participation. A total of 51 patients (37 females and 14 males) with studies performed at 3 time points were included in this study. For patients with multiple aneurysms, we only analyzed flow into the largest one.

MR protocol

A 1.5T MR (Achieva, Philips Medical System, Best, The Netherlands) with a 6-channel head coil was used in this study. First, a three-dimensional contrast-enhanced MRA (CE-MRA) sequence was acquired following institutional clinical practice. A weight-adjusted single dose of GdDTPA diluted with saline to a 20mL volume was injected and was followed by 15 mL of saline all delivered at 2 mL/s. The CE-MRA sequence used elliptic-centric phase reordering, and data were acquired using parallel imaging with an acceleration factor of 2. Imaging parameters included the following: TR/TE/flip angle×5/2/30°. Images were acquired from a 54-mm paracoronal slab, with a FOV of 240 mm and an acquisition matrix of 400 × 380 × 45 zero-filled to 512 × 512 × 90. The resultant images had a resolution of 0.6 × 0.63 × 1.2 mm3 and was interpolated to 0.47 × 0.47 × 0.6 mm3. Total acquisition time was of the order of 35 seconds.

MIP images reconstructed from the CE-MRA data were used to localize the aneurysm and its feeding arteries. The 2D through-plane velocity-encoded sequence was then oriented in a plane transverse to the feeding artery using two orthogonal views (Fig 1 A) and velocity encoding was prescribed for through plane flow with the encoding gradient perpendicular to the image plane. To facilitate measurement, the 2D through-plane was placed at least 5 times of the inlet diameter from the proximal of the aneurysm at a relative straight segment without stenosis. Data was acquired using a finger pulse monitor with retrospective gating. Acquisition parameters were as follows: TR/TE/flip angle=8/5/15°. FOV 160×160mm with a slice thickness of 5mm. Velocity encoding (VENC) was set to 100cm/s. The acquisition matrix was 160×160, and the images were reconstructed to a 0.6×0.6mm resolution. The data was retrospectively triggered, and reconstructed to either 15 or 32 time frames, providing the time-varying inlet boundary conditions required for the pulsatile flow simulations.

Post-processing

A research Graphical User Interface (GUI) software Segment (2.2R7056)[16] was used to draw the regions of interest and extract velocity information. First, an elliptic region of interest was roughly drawn around the inlet artery using the magnitude image from the PCMR data; second, an automatic tracking and refinement function was used to refine the regions of interest across all phases (Fig. 1 B, C). The final ROIs were independent of the

Author Manuscript Author Manuscript Author Manuscript Author Manuscript

initial contour and further reviewed by 2 Neuroradiologists; discrepancy was resolved by discussion. third, flow values were measured at each time point through the entire cardiac cycle (Fig. 1D, E). The time-averaged flow rate through the cardiac cycle (mean flow (MF)), flow at peak systole (max flow (MAF)), flow at end diastole (min flow (MIF)), peak systolic velocity (max velocity (MAV)), end-diastolic velocity (min velocity (MIV)), velocity averaged over the whole cycle (mean velocity (MV)), and the area of the region of interest (ROI) were extracted for further analysis.

CFD Simulation

The 3D geometry of the intracranial aneurysms was segmented and reconstructed from CE-MRA using Mimics 20.0(Materialise NV, Leuven, Belgium). The surface was remeshed to an edge size of 0.4 mm and then smoothed while preserving the shape using Geomagic DesignX (Geomagic, Research Triangle Park, NC, USA)[17]. An inlet vessel length of at least four diameters of the parent artery was incorporated to ensure fully developed flow[18]. The models were meshed in Ansys with a mixture of prism and tetrahedral elements. As previously reported[19,20], grid size verification ranging from 0.4 to 0.1 mm was performed on 2 randomly selected patients using steady flow. The difference in average wall shear stress (WSS) was calculated and the maximum grid size was selected to provide a difference in WSS smaller than 5% - which was for a grid size of 0.2mm.

CFD transient simulations were performed three times in 10 aneurysms, once with the inlet waveform obtained from PCMR and the other with an inlet waveform either artificially elevated or reduced (where an increase or decrease in flow was enforced at every time point through the cardiac cycle) as the inlet boundary condition. The outlet pressure was set to 0 Pa. Blood was simulated as a Newtonian fluid with a density of 1060kg/m3 and dynamic viscosity of 0.0035 Pa.s, respectively. The simulation was performed using Fluent's pressure-based solver with the DOUBLE pressure-velocity coupling scheme. The CFD convergence criteria were set at 0.001 for the continuity and velocity residuals. Three cardiac cycles were performed for each patient, the data of the last cardiac cycle was saved for visualization and statistical analysis.

CFD post-processing was performed with paraview 5.6 (Kitware, Clifton Park, NY) and python 3.7 (https://www.python.org/). Systolic WSS, diastolic WSS, time-averaged wall shear stress (TAWSS) and low wall shear stress area (LSA) were each calculated. LSA is defined as the percentage of the aneurysm area where the WSS is 1 SD below the mean WSS in the parent artery (within 1cm of centerline node at the aneurysm neck)[21]. A point-by-point comparison of WSS and LSA was made between the different simulated flow conditions.

Statistical analysis

Statistical analysis was performed using Python 3.7. All measurement data are presented as Mean ± standard deviation, enumeration data is presented in percentages. The intraclass correlation coefficient (ICC) and Coefficient of Variance (CV) of MF, MAF, MIF, MV, MAV, MIV and ROI area of each artery was calculated. The mean value of 51 patients was used to characterize the variation of the included parameters. Bland-Altman plots were

Author Manuscript Author Manuscript Author Manuscript Author Manuscript

performed to analyze the agreement among 3 time points. A T-test or Wilcoxon test was performed to compare the difference between the two groups. A p-value of 0.05 was selected as the threshold for statistical significance.

Results

The average age of the 51 included patients was 62±16 years. 29 aneurysms were located on an internal carotid artery (ICA), 11 were located on the basilar artery (BA), 6 on the vertebral artery (VA), 3 at the anterior communicating artery (ACA), and 2 on the middle cerebral artery (MCA). The average time interval between sequential studies was 0.64±0.21 years.

Normal ranges

The mean value, the standard deviation of MF, MAF, MIF, MV, MAV, MIV and ROI area are presented in Table 1. The distributions of investigated parameters across different artery segments are displayed in online-fig1. The largest ROI area was in the ICA and the smallest in the ACA.

Intra-Individual Variation

The overall reproducibility for all the parameters included is shown in Table 2. The limits of agreement of 3 measurements are plotted in Fig 2. The ICCs are excellent for MF, MAF, MIF, MV, MAV, and ROI. The CV is larger in MIF than in MF and MAF (0.16 vs. 0.10 and 0.11, p=0.007 and p=0.01). Similarly, the CV is larger in MIV than MV and MAV (0.18 vs. 0.12 and 0.12, p=0.02 and p=0.01). The Histogram of frequency distribution of flow and velocity parameters is shown in online-fig 2. The CV distribution of flow and velocity parameters based on artery locations is shown in online-fig 3. The CV of ROI-area is 11%. The median area size of 0.15 cm^2 was selected as a cutoff value for dividing the aneurysms into two groups. A T test showed that there is no significant difference in the CV of MF between the group with a larger ROI area than the group with a smaller ROI area. (p=0.88).

Influence of flow variance on CFD results

CFD simulations were performed three times in the 10 aneurysms from 5 locations, once with the measured flow waveform and then, to assess the effect of typical measurement inaccuracy, with artificially elevated or reduced flow waveform (of +10% or −10% based on these experimentally measured CV of MF) as the inlet boundary condition, to explore their impact on CFD derived flow metrics. The aneurysm information and simulation results are summarized in table 3 and demonstrated in Fig 3. A 10% error in flow resulted in a number of hemodynamic changes including: 41.41% of WSS at systolic phase, 39.13% of WSS at diastolic phase, 2.79% of LSA at systolic phase, 2.12% of LSA at diastolic phase, 47.57% of TAWSS and 0.17% of oscillatory shear index (OSI).

Discussion

In this study, we determined the variability over time of flow and velocity parameters derived from 2D PCMR for patients with unruptured intracranial aneurysms where these

Author Manuscript Author Manuscript Author Manuscript Author Manuscript

patients were examined at 3-time points in follow-up. We found a wide range and generally good reproducibility for the flow and velocity parameters. We then examined the impact of this variability in computed hemodynamic descriptors when the original flow waveforms and artificially elevated flow waveforms (original flow plus variation) were used as inlet boundary conditions in CFD calculations. The results indicate that 10% variation in intra-individual flow could lead to a difference of around 40% in WSS but only around 2.5% in LSA. The result suggests that we should be cautious when we use absolute value of WSS in the evaluation of aneurysm growth or rupture risks, on a patient specific basis.

Normal flow and velocity distribution have been reported previously[15,22]. The reported mean flow and velocity were generally of the order of 10% to 20% greater than the mean flow in our study. A number of factors might contribute to these discrepancies such as magnetic field strength, methods for defining the ROI area[23], and patient age[24]. Given that the population in our study is older (62±16 years) than in these studies, it is likely that age is the major contributor to this discrepancy.

The reproducibility and variation of 2D flow in the intracranial arteries has been reported in previous studies[25,22,26,27]. Taviani et al reported that the CV of MF in the aorta is about 0.107 in 9 volunteers[28]. Aart et al reported the CV of repeated total CBF measurement is about 11% in 15 volunteers[27]. Our study found a similar result for CV based on a large dataset over a long-term follow-up (mean 2.1 years). The overall reproducibility of MF and velocity parameters was good even though measurements were repeated with long (>6 months) intervals between studies. The improved determination of reproducibility in our study could be attributed to three reasons: first, a strict methodology was employed to specify the plane perpendicular to the inlet vessel; second, the ROI was drawn with an automated refinement tool; third, we have a larger sample size and number of follow up time points. We also compared the CV of flow between arteries with large area size and arteries with small area size. Results showed that CV is independent of artery area size. All these results indicate that PCMR measurements are reliable, and that the flow conditions in these aneurysm patients is fairly stable.

CFD has played an important role in intracranial aneurysm research. Specification of inlet boundary conditions have evolved from generalized and idealized flow values to patient-specific flow conditions[29,12,30]. A comparison of simulation results showed that both aneurysm WSS magnitude and WSS distribution was different depending on whether generalized flow or patient-specific flow was specified[12]. In our longitudinal study with a relatively large dataset, we showed that the CV of MF is about 10%. We further verified the effect of flow error on computed WSS. A 10% variation in flow was found to generate of the order of a 20% change in WSS, but only a 4%-5% change in LSA and OSI. The determination of the distribution of WSS is likely of high importance in aneurysm evolution. Specifically, we have previously reported aneurysm growth is co-located with areas of LSA[5]. These findings suggest that we should be cautious about the absolute value of WSS, when we interpret the results of a patient specific CFD calculation. However, the LSA and OSI might be reliable tools for evaluating aneurysm growth or rupture risks when a patient-specific inlet boundary flow waveform condition is used.

Author Manuscript Author Manuscript Author Manuscript Author Manuscript

There are additional limitations to this study. First, since this is an intracranial aneurysm patient cohort, more data was acquired for locations in the ICA and BA than other territories, since the measurements were performed to determine inlet flow velocities in the parent vessels of intracranial aneurysms, and these locations were the sites of highest prevalence of aneurysms in this study. Second, the time interval between each repeated study is longer than in typical reproducibility studies. Although this implies that measurements in a narrower time interval might yield more accurate estimates of reproducibility, it also would suggest that measurement reproducibility might be even better than what we report. Third, our study used 2D PCMR which only obtained the through-plane flow information. In recent years, the use of 4D Flow imaging which enables full coverage of the intracranial vasculature has gained increased interest[31,19]. However, those studies require much longer scan times (~12 minutes) than a single 2D PCMR acquisition (~30 secs) and are therefore subject to patient motion, and are difficult to accommodate in routine clinical practice. Fourth, our study used a 1.5T MR system. While the influence of magnetic field strength on flow measurement remains unclear, a higher magnetic field strength of 3T or 7T would offer higher SNR, an improved velocity to noise ratio, and likely a better ability to delineate the ROI. Fifth, we directly used a post-contrast PC-MRI, the influence of residual Gd on PC-MRI was not evaluated here. Sixth, in this study, we selected saccular aneurysms for CFD analysis that were representative of the larger set of aneurysms that we have analyzed. However, aneurysm geometry type may lead to different sensitivity to flow variation, and the possible geometric configurations is extremely large. Future studies with larger sample size should be performed to focus on this variability. Seventh, it would be preferable in future simulations, to include a greater length of patient-specific vascular geometry proximal to the inlet location to generate inlet boundary conditions that are even closer to the real physiological conditions.

In conclusion, this study identified that intra-individual MF, as measured by PCMR, varied by an amount of the order of 10%. A 10% variation in flow was found to generate of the order of a 40% change in WSS, but only a 2.5% change in LSA and 0.17% change in OSI. These findings suggest that we should be cautious about the absolute value of WSS, when interpreting the results of a patient specific CFD calculation. However, the LSA and OSI might be reliable metrics for evaluating aneurysm growth or rupture risks when a patient-specific inlet boundary flow waveform condition is used.

Supplementary Material

Refer to Web version on PubMed Central for supplementary material.

Acknowledgments

Funding:

This work was supported by research award NS059944 (DS) from the NIH.

Compliance with ethical standards

The authors declare no conflict of interest.

Author Manuscript Author Manuscript Author Manuscript Author Manuscript

The institutional review board of the University of California San Francisco approved this study (reference number: 10-03060). All human subjects involved gave informed written consent for study participation.

Reference

1. Go AS, Mozaffarian D, Roger VL, Benjamin EJ, Berry JD, Blaha MJ, Dai S, Ford ES, Fox CS, Franco S, Fullerton HJ, Gillespie C, Hailpern SM, Heit JA, Howard VJ, Huffman MD, Judd SE, Kissela BM, Kittner SJ, Lackland DT, Lichtman JH, Lisabeth LD, Mackey RH, Magid DJ, Marcus GM, Marelli A, Matchar DB, McGuire DK, Mohler ER 3rd, Moy CS, Mussolino ME, Neumar RW, Nichol G, Pandey DK, Paynter NP, Reeves MJ, Sorlie PD, Stein J, Towfighi A, Turan TN, Virani SS, Wong ND, Woo D, Turner MB (2014) Heart disease and stroke statistics--2014 update: a report from the American Heart Association. Circulation 129 (3):e28–e292. [PubMed: 24352519]
2. Morita A, Kirino T, Hashi K, Aoki N, Fukuhara S, Hashimoto N, Nakayama T, Sakai M, Teramoto A, Tominari S, Yoshimoto T (2012) The natural course of unruptured cerebral aneurysms in a Japanese cohort. The New England journal of medicine 366 (26):2474–2482. [PubMed: 22738097]
3. Wiebers DO, Whisnant JP, Huston J 3rd, Meissner I, Brown RD Jr., Piepgras DG, Forbes GS, Thielen K, Nichols D, O'Fallon WM, Peacock J, Jaeger L, Kassell NF, Kongable-Beckman GL, Torner JC (2003) Unruptured intracranial aneurysms: natural history, clinical outcome, and risks of surgical and endovascular treatment. Lancet 362 (9378):103–110. [PubMed: 12867109]
4. Rayz VL, Abla A, Boussel L, Leach JR, Acevedo-Bolton G, Saloner D, Lawton MT (2015) Computational Modeling of Flow-Altering Surgeries in Basilar Aneurysms. Annals of biomedical engineering 43 (5):1210–1222. [PubMed: 25348846]
5. Boussel L, Rayz V, McCulloch C, Martin A, Acevedo-Bolton G, Lawton M, Higashida R, Smith WS, Young WL, Saloner D (2008) Aneurysm growth occurs at region of low wall shear stress: patient-specific correlation of hemodynamics and growth in a longitudinal study. Stroke 39 (11):2997–3002. [PubMed: 18688012]
6. Jou LD, Wong G, Dispensa B, Lawton MT, Higashida RT, Young WL, Saloner D (2005) Correlation between lumenal geometry changes and hemodynamics in fusiform intracranial aneurysms. AJNR American journal of neuroradiology 26 (9):2357–2363. [PubMed: 16219845]
7. Meng H, Tutino VM, Xiang J, Siddiqui A (2014) High WSS or low WSS? Complex interactions of hemodynamics with intracranial aneurysm initiation, growth, and rupture: toward a unifying hypothesis. AJNR American journal of neuroradiology 35 (7):1254–1262. [PubMed: 23598838]
8. Khan MO, Steinman DA, Valen-Sendstad K (2017) Non-Newtonian versus numerical rheology: Practical impact of shear-thinning on the prediction of stable and unstable flows in intracranial aneurysms. International journal for numerical methods in biomedical engineering 33 (7).
9. Cebral JR, Duan X, Chung BJ, Putman C, Aziz K, Robertson AM (2015) Wall Mechanical Properties and Hemodynamics of Unruptured Intracranial Aneurysms. AJNR American journal of neuroradiology 36 (9):1695–1703. [PubMed: 26228891]
10. Berg P, Voss S, Saalfeld S, Janiga G, Bergersen AW, Valen-Sendstad K, Bruening J, Goubergrits L, Spuler A, Cancelliere NM, Steinman DA, Pereira VM, Chiu TL, Tsang ACO, Chung BJ, Cebral JR, Cito S, Pallares J, Copelli G, Csippa B, Paal G, Fujimura S, Takao H, Hodis S, Hille G, Karmonik C, Elias S, Kellermann K, Khan MO, Marsden AL, Morales HG, Piskin S, Finol EA, Pravdivtseva M, Rajabzadeh-Oghaz H, Paliwal N, Meng H, Seshadhri S, Howard M, Shojima M, Sugiyama SI, Niizuma K, Sindeev S, Frolov S, Wagner T, Brawanski A, Qian Y, Wu YA, Carlson KD, Dragomir-Daescu D, Beuing O (2018) Multiple Aneurysms AnaTomy CHallenge 2018 (MATCH): Phase I: Segmentation. Cardiovasc Eng Technol 9 (4):565–581. [PubMed: 30191538]
11. Voss S, Beuing O, Janiga G, Berg P (2019) Multiple Aneurysms AnaTomy CHallenge 2018 (MATCH)-Phase Ib: Effect of morphology on hemodynamics. PloS one 14 (5):e0216813. [PubMed: 31100101]
12. Jansen IG, Schneiders JJ, Potters WV, van Ooij P, van den Berg R, van Bavel E, Marquering HA, Majoie CB (2014) Generalized versus patient-specific inflow boundary conditions in computational fluid dynamics simulations of cerebral aneurysmal hemodynamics. AJNR American journal of neuroradiology 35 (8):1543–1548. [PubMed: 24651816]

Author Manuscript Author Manuscript Author Manuscript Author Manuscript

13. Stalder AF, Russe MF, Frydrychowicz A, Bock J, Hennig J, Markl M (2008) Quantitative 2D and 3D phase contrast MRI: optimized analysis of blood flow and vessel wall parameters. Magnetic resonance in medicine 60 (5):1218–1231. [PubMed: 18956416]

14. Leach JR, Rayz VL, Soares B, Wintermark M, Mofrad MR, Saloner D (2010) Carotid atheroma rupture observed in vivo and FSI-predicted stress distribution based on pre-rupture imaging. Annals of biomedical engineering 38 (8):2748–2765. [PubMed: 20232151]

15. Correia de Verdier M, Wikstrom J (2016) Normal ranges and test-retest reproducibility of flow and velocity parameters in intracranial arteries measured with phase-contrast magnetic resonance imaging. Neuroradiology 58 (5):521–531. [PubMed: 26882908]

16. Heiberg E, Sjogren J, Ugander M, Carlsson M, Engblom H, Arheden H (2010) Design and validation of Segment--freely available software for cardiovascular image analysis. BMC medical imaging 10:1. [PubMed: 20064248]

17. Rayz VL, Boussel L, Acevedo-Bolton G, Martin AJ, Young WL, Lawton MT, Higashida R, Saloner D (2008) Numerical Simulations of Flow in Cerebral Aneurysms: Comparison of CFD Results and In Vivo MRI Measurements. Journal of biomechanical engineering 130 (5):051011–051011–051019. [PubMed: 19045518]

18. Hoi Y, Wasserman BA, Lakatta EG, Steinman DA (2010) Effect of Common Carotid Artery Inlet Length on Normal Carotid Bifurcation Hemodynamics. Journal of biomechanical engineering 132 (12).

19. Boussel L, Rayz V, Martin A, Acevedo-Bolton G, Lawton MT, Higashida R, Smith WS, Young WL, Saloner D (2009) Phase-contrast magnetic resonance imaging measurements in intracranial aneurysms in vivo of flow patterns, velocity fields, and wall shear stress: comparison with computational fluid dynamics. Magnetic resonance in medicine 61 (2):409–417. [PubMed: 19161132]

20. Boussel L, Wintermark M, Martin A, Dispensa B, VanTijen R, Leach J, Rayz V, Acevedo-Bolton G, Lawton M, Higashida R, Smith WS, Young WL, Saloner D (2008) Monitoring Serial Change in the Lumen and Outer Wall of Vertebrobasilar Aneurysms. American Journal of Neuroradiology 29 (2):259–264. [PubMed: 17974611]

21. Brinjikji W, Chung BJ, Jimenez C, Putman C, Kallmes DF, Cebral JR (2017) Hemodynamic differences between unstable and stable unruptured aneurysms independent of size and location: a pilot study. Journal of neurointerventional surgery 9 (4):376–380. [PubMed: 27048958]

22. Zhao M, Amin-Hanjani S, Ruland S, Curcio AP, Ostergren L, Charbel FT (2007) Regional cerebral blood flow using quantitative MR angiography. AJNR American journal of neuroradiology 28 (8):1470–1473. [PubMed: 17846193]

23. Cebral JR, Castro MA, Putman CM, Alperin N (2008) Flow-area relationship in internal carotid and vertebral arteries. Physiol Meas 29 (5):585–594. [PubMed: 18460763]

24. Mitchell GF, van Buchem MA, Sigurdsson S, Gotal JD, Jonsdottir MK, Kjartansson O, Garcia M, Aspelund T, Harris TB, Gudnason V, Launer LJ (2011) Arterial stiffness, pressure and flow pulsatility and brain structure and function: the Age, Gene/Environment Susceptibility--Reykjavik study. Brain 134 (Pt 11):3398–3407. [PubMed: 22075523]

25. Enzmann DR, Ross MR, Marks MP, Pelc NJ (1994) Blood flow in major cerebral arteries measured by phase-contrast cine MR. American Journal of Neuroradiology 15 (1):123–129. [PubMed: 8141043]

26. HOPPE M, HEVERHAGEN JT, FROELICH JJ, KUNISCH-HOPPE M, KLOSE K-J, WAGNER H-J (1998) Correlation of Flow Velocity Measurements By Magnetic Resonance Phase Contrast Imaging and Intravascular Doppler Ultrasound. Investigative radiology 33 (8):427–432. [PubMed: 9704280]

27. Spilt A, Box FMA, van der Geest RJ, Reiber JHC, Kunz P, Kamper AM, Blauw GJ, van Buchem MA (2002) Reproducibility of total cerebral blood flow measurements using phase contrast magnetic resonance imaging. Journal of Magnetic Resonance Imaging 16 (1):1–5. [PubMed: 12112496]

28. Taviani V, Patterson AJ, Graves MJ, Hardy CJ, Worters P, Sutcliffe MPF, Gillard JH (2010) Accuracy and repeatability of fourier velocity encoded M-mode and two-dimensional cine phase contrast for pulse wave velocity measurement in the descending aorta. Journal of Magnetic Resonance Imaging 31 (5):1185–1194. [PubMed: 20432355]

Author Manuscript Author Manuscript Author Manuscript Author Manuscript

29. Sun Q, Groth A, Aach T (2012) Comprehensive validation of computational fluid dynamics simulations of in-vivo blood flow in patient-specific cerebral aneurysms. Medical physics 39 (2):742–754. [PubMed: 22320784]

30. Onishi Y, Aoki K, Amaya K, Shimizu T, Isoda H, Takehara Y, Sakahara H, Kosugi T (2013) Accurate determination of patient-specific boundary conditions in computational vascular hemodynamics using 3D cine phase-contrast MRI. International journal for numerical methods in biomedical engineering 29 (10):1089–1103. [PubMed: 23733738]

31. Bollache E, van Ooij P, Powell A, Carr J, Markl M, Barker AJ (2016) Comparison of 4D flow and 2D velocity-encoded phase contrast MRI sequences for the evaluation of aortic hemodynamics. The international journal of cardiovascular imaging 32 (10):1529–1541. [PubMed: 27435230]

Author Manuscript
Author Manuscript
Author Manuscript
Author Manuscript

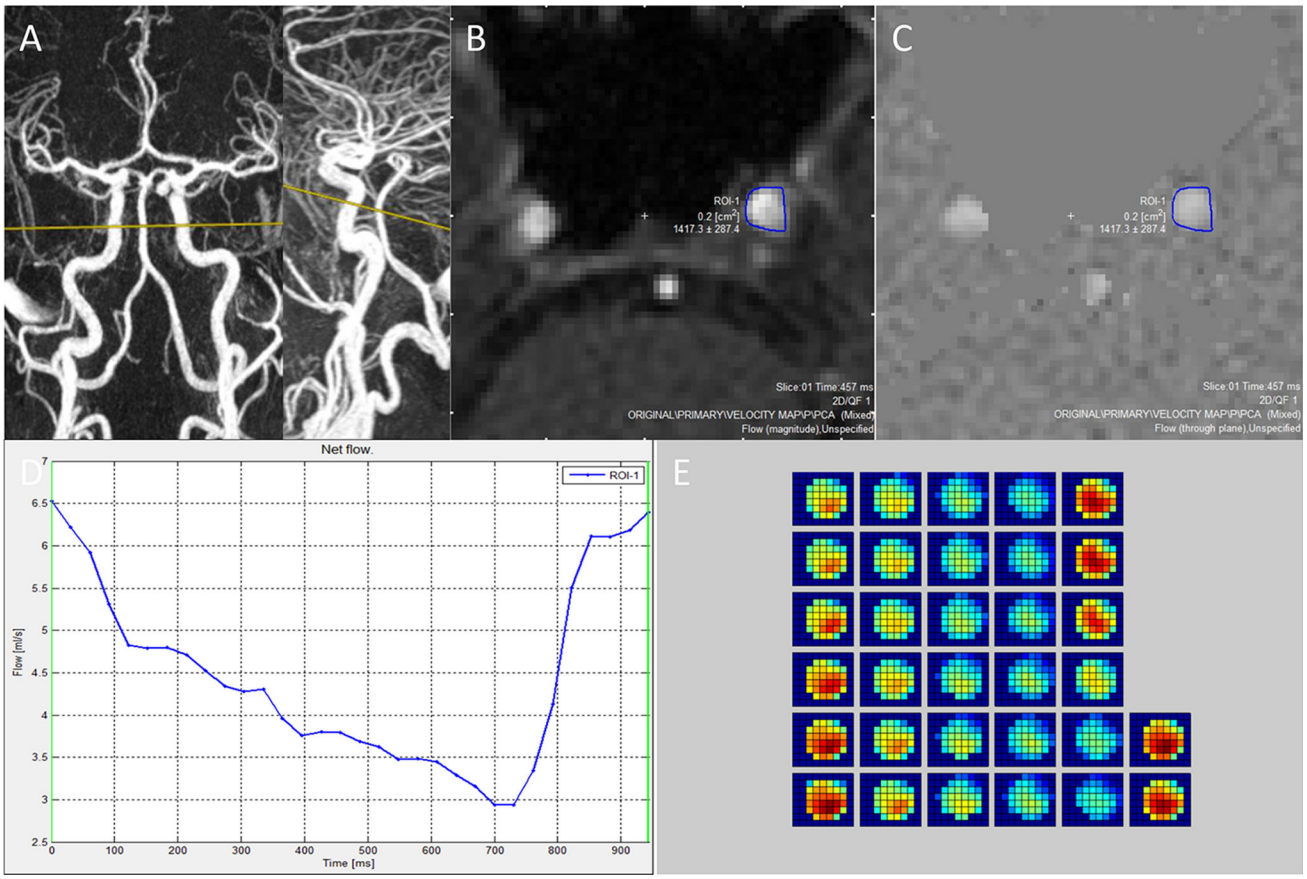

Fig. 1.

Placement of 2D PC plane, ROI contouring and flow information extraction for a patient with an aneurysm of the left ICA. A) MIP image of CE-MRA; yellow line on anterior-posterior and lateral view shows the position of perpendicular plane at C2 segment; ROI on B) magnitude and C) phase image after automatic refinement; D) net flow plot through entire cardiac cycle; E) velocity values from 32 phases of one cardiac cycle which is consistent with a generally parabolic velocity distribution.

Author Manuscript Author Manuscript Author Manuscript Author Manuscript

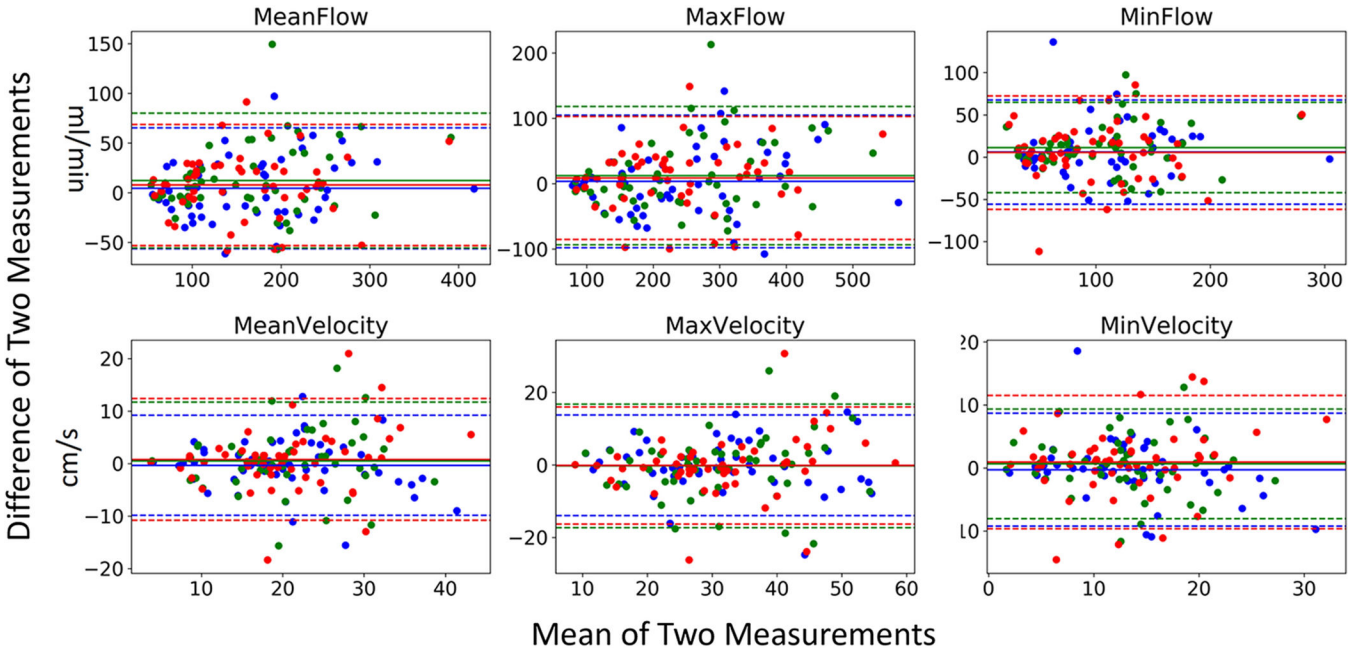

Fig 2.

Bland Altman plots for flow and velocity parameters for paired comparisons from 3 time points. Horizontally, the average of the two measurements is plotted, and vertically, the difference of these two measurements. Middle dash line: mean difference; upper and lower dash line: limit of agreement (mean ± 1.96 standard deviation, the range between the lines represents least detectable difference). Blue: measurement agreement between first and second time point; Green: measurement agreement between first and third time point; Red: measurement agreement between second and third time point.

Author Manuscript Author Manuscript Author Manuscript Author Manuscript

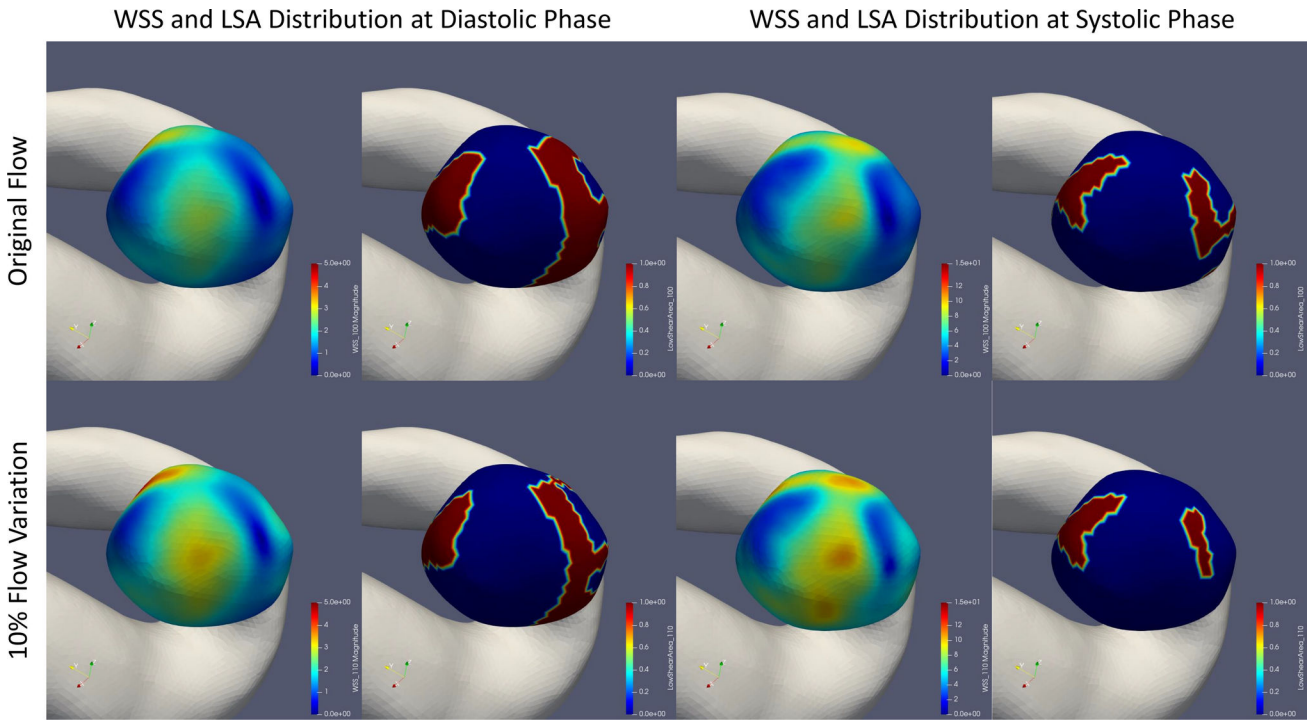

Fig 3.

Example of computed WSS and LSA distribution on diastolic and systolic phase assuming a 10% variation in flow.

Author Manuscript

Author Manuscript

Author Manuscript

Author Manuscript

Table 1

the range of flow, velocity parameters, and ROI at different locations.

	MeanFlow (ml/min)	MaxFlow (ml/min)	MinFlow (ml/min)	MeanVelocity (cm/s)	MinVelocity (cm/s)	MaxVelocity (cm/s)	RoiArea (cm^2)
ICA	204.91±57.25	306.77±83.06	132.68±41.51	21.99±5.15	14.41±3.94	32.87±7.82	0.16±0.04
VA	70.84±20.19	108.92±31.59	42.26±14.65	13.65±3.08	8.11±1.68	21.51±5.02	0.1±0.06
BA	112.75±11.52	156.76±24.26	53.49±12.65	14.0±8.9	8.17±5.89	23.87±12.18	0.15±0.08
MCA	124.5±7.02	207.11±9.1	76.86±6.2	29.0±0.5	18.56±0.35	44.69±3.39	0.07±0.01
ACA	93.67±23.25	133.27±28.72	60.69±17.91	29.08±10.48	20.14±8.67	41.19±13.5	0.06±0.01

ICA, internal carotid artery; VA, vertebral artery; BA, basilar artery; MCA, middle cerebral artery; ACA, anterior cerebral artery. ROI, region of interest.

Author Manuscript

Author Manuscript

Author Manuscript

Author Manuscript

Table 2

Reproducibility and Variation of included parameters

	Mean CV	ICC	0.95 confidence interval	p
MeanFlow	0.10 ± 0.06	0.90	[0.85, 0.94]	<0.01
MaxFlow	0.11 ± 0.06	0.90	[0.83, 0.93]	<0.01
MinFlow	0.16 ± 0.14	0.83	[0.75, 0.89]	<0.01
MeanVelocity	0.12 ± 0.09	0.79	[0.69, 0.86]	<0.01
MinVelocity	0.18 ± 0.16	0.71	[0.59, 0.81]	<0.01
MaxVelocity	0.12 ± 0.08	0.77	[0.67, 0.85]	<0.01
RoiArea	0.11 ± 0.08	0.84	[0.76, 0.90]	<0.01

CV, coefficient of variance; ICC, intraclass correlation coefficient; ROI, region of interest.

Author Manuscript

Author Manuscript

Author Manuscript

Author Manuscript

Table 3

The change in computed WSS, LSA, TAWSS, and OSI assuming a +/− 10% flow error.

	Adding 10% Flow	Reducing 10% Flow	Mean 10% Flow Variation
Diastolic WSS Change	26.27%	56.56%	41.41%
Systolic WSS Change	28.51%	49.74%	39.13%
Diastolic LSA Change	0.61%	4.97%	2.79%
Systolic LSA Change	0.72%	3.52%	2.12%
TAWSS Change	59.12%	36.03%	47.57%
OSI Change	0.19%	0.15%	0.17%

WSS, wall shear stress; LSA, low wall shear stress area; TAWSS, time-averaged wall shear stress; OSI, oscillatory shear index.